Hyperfine Structure and g_J Value of the $^2D_{3/2}$ and of the $^4F_{9/2}$ States of Au^{197}

Arthur G. Blachman,* Donald A. Landman,† and Allen Lurio

IBM Watson Laboratory, Columbia University, New York, New York

(Received 15 March 1967)

The hyperfine structure (hfs) and g_J value of the metastable $(5d^96s^2)$ $^2D_{3/2}$ and of the $(5d^96s6p)$ $^4F_{9/2}$ levels in Au^{197} have been measured by the atomic-beam magnetic-resonance method. The results for the hfs interaction constants, which have been corrected for second-order interactions with neighboring fine-structure levels, are $A(^2D_{3/2}) = 199.8425(2)$ Mc/sec, $B(^2D_{3/2}) = -911.0766(5)$ Mc/sec, $C(^2D_{3/2}) = 0.000212(14)$ Mc/sec, $A(^4F_{9/2}) = 432.276(1)$ Mc/sec, $B(^4F_{9/2}) = -540.026(17)$ Mc/sec, and $C(^4F_{9/2}) = 0.00326(10)$ Mc/sec. A detailed interpretation of these measurements together with those of Goodman and Childs on the $(5d^96s^2)$ $^2D_{5/2}$ level yields a value for the quadrupole moment of $Q = 0.594(10)$ b without the Sternheimer correction. We are not able to obtain a consistent value for the octupole moment. From the Zeeman effect of the hfs we find $g_J(^2D_{3/2}) = 0.799(1)$ and $g_J(^4F_{9/2}) = 1.334(2)$.

I. INTRODUCTION

THIS is the second of three papers dealing with the hyperfine structure of several metastable electronic levels in the naturally occurring isotopes of the group Ib elements.[1] The measurements were made by the atomic-beam magnetic-resonance method. In this paper, we present the results and interpretation of the hyperfine structure of the $(5d^96s^2)$ $^2D_{3/2}$ and the $(5d^96s6p)$ $^4F_{9/2}$ levels in Au^{197} $(I = \frac{3}{2})$.[2]

The details of the apparatus have been described in previous papers.[3] Briefly, the metastable atoms in the beam were produced by cross-electron bombardment of the ground-state beam. The source of the ground-state beam was a cylindrical Mo oven with an inner graphite crucible, heated to ~1750°C by means of electron bombardment. The metastable atoms were detected by causing the refocused beam to strike a Cs-coated surface and then collecting the electrons produced by the resulting Auger de-excitation of the metastable atoms. The detector is sensitive only to the metastable components of the beam which have excitation energies $\gtrsim 1.8$ eV (the Cs work function).

II. THEORY

We will write the hfs interaction Hamiltonian as

$$\mathcal{H}_{\text{hfs}} = \sum_k T_e^{(k)} \cdot T_n^{(k)} \quad \text{with} \quad T_e^{(k)} = \sum_i T_e^{(k)}(i), \quad (1)$$

where the i summation is over all electrons and the tensor operators $T_e^{(k)}$ and $T_n^{(k)}$ operate on the space

of electron and nuclear coordinates, respectively.[4] Since $I = \frac{3}{2}$ for Au^{197}, we will need only the operators for which $k = 1$, 2, and 3. These nuclear operators are related to the nuclear moments by

$$\mu_I = \langle \beta\tfrac{3}{2}\tfrac{3}{2} \mid T_n^{(1)}{}_0 \mid \beta\tfrac{3}{2}\tfrac{3}{2} \rangle = \text{magnetic dipole moment},$$

$$Q = \frac{2}{e} \langle \beta\tfrac{3}{2}\tfrac{3}{2} \mid T_n^{(2)}{}_0 \mid \beta\tfrac{3}{2}\tfrac{3}{2} \rangle = \text{electric quadrupole moment},$$

$$\Omega = - \langle \beta\tfrac{3}{2}\tfrac{3}{2} \mid T_n^{(3)}{}_0 \mid \beta\tfrac{3}{2}\tfrac{3}{2} \rangle = \text{magnetic octupole moment},$$

where $\mid \beta\tfrac{3}{2}\tfrac{3}{2} \rangle$ denotes the nuclear state with $m_I = \frac{3}{2}$ and β signifies all other quantum numbers needed to specify the nuclear state.

Using Eq. (1) together with a set of zero-order wave functions $\mid \beta\tfrac{3}{2}\alpha JFm_F \rangle$ (α denotes all other quantum numbers needed to specify the electronic state of the atom) we can write the hfs term energy to second order in a perturbation expansion as

$$W_F = W_F{}^{(1)} + W_F{}^{(2)} = hA(\alpha J)\tfrac{1}{2}K$$

$$+ hB(\alpha J) \frac{[K(K+1) - 5J(J+1)]}{8J(2J-1)} + hC(\alpha J)$$

$$\times \frac{5K^3 + 20K^2 + K[-41J(J+1)+27] - 75J(J+1)}{6J(J-1)(2J-1)}$$

$$+ W_F{}^{(2)}, \quad (2)$$

where

$$K = F(F+1) - J(J+1) - \tfrac{15}{4},$$

$$A(\alpha J) = (2\mu_I/3J)\langle \alpha JJ \mid T_e^{(1)}{}_0 \mid \alpha JJ \rangle,$$

$$B(\alpha J) = 2eQ\langle \alpha JJ \mid T_e^{(2)}{}_0 \mid \alpha JJ \rangle,$$

and

$$C(\alpha J) = -\Omega\langle \alpha JJ \mid T_e^{(3)}{}_0 \mid \alpha JJ \rangle$$

are the magnetic-dipole, electric-quadrupole, and magnetic-octupole hfs interaction constants, respectively. In the above equations we have taken $I = \frac{3}{2}$ explicitly. In cases where there are levels of the same F value

---

* Present Address: IBM Research Center, Yorktown Heights, New York.

† Present Location: New York University, University Heights, Bronx, New York.

[1] The first paper was A. G. Blachman, D. A. Landman, and A. Lurio, Phys. Rev. 150, 59 (1966).

[2] A. G. Blachman and A. Lurio, Bull. Am. Phys. Soc. 8, 9 (1963); D. A. Landman, A. G. Blachman, and A. Lurio, Brookhaven Conference on Molecular and Atomic Resonance, Uppsala, Sweden, 1964 (unpublished).

[3] See Ref. 1 and also A. Lurio, Phys. Rev. 126, 1768 (1962).

[4] The presentation of the theory follows that developed by C. Schwartz, Phys. Rev. 97, 380 (1955); 105, 173 (1957).

arising from other nearby fine-structure levels, the second-order term $W_F{}^{(2)}$ may contribute significantly to the energy. Explicitly, we have

$$W_F{}^{(2)}= \sum_{(\alpha'J')}{}' |\langle \beta\tfrac{3}{2}\alpha JFm | \mathfrak{IC}_{\mathrm{hfs}} | \beta\tfrac{3}{2}\alpha'J'Fm\rangle|^2 [W(\alpha J)-W(\alpha'J')]^{-1}$$

$$= \sum_{(\alpha'J')}{}' \Bigg[\sum_{k_1,k_2} \begin{Bmatrix} \tfrac{3}{2} & J' & F \\ J & \tfrac{3}{2} & k_1 \end{Bmatrix} \begin{Bmatrix} \tfrac{3}{2} & J' & F \\ J & \tfrac{3}{2} & k_2 \end{Bmatrix} \times \langle \beta\tfrac{3}{2} \| T_n{}^{(k_1)} \| \beta\tfrac{3}{2} \rangle \langle \beta\tfrac{3}{2} \| T_n{}^{(k_2)} \| \beta\tfrac{3}{2} \rangle \langle \alpha J \| T_e{}^{(k_1)} \| \alpha'J' \rangle$$

$$\times \langle \alpha J \| T_e{}^{(k_2)} \| \alpha'J' \rangle \Bigg] [W(\alpha J)-W(\alpha'J')]^{-1},$$

where $W(\alpha J)-W(\alpha'J')$ is the fine-structure separation and the prime on the summation means that $\alpha'J'\neq\alpha J$. Since $\langle \beta I \| T_n{}^{(3)} \| \beta I \rangle \langle \alpha J \| T_e{}^{(3)} \| \alpha J \rangle \ll \langle \beta I \| T_n{}^{(1)} \| \beta I \rangle \langle \alpha J \| T_e{}^{(1)} \| \alpha J \rangle$ and $\langle \beta I \| T_n{}^{(2)} \| \beta I \rangle \langle \alpha J \| T_e{}^{(2)} \| \alpha J \rangle$, only the terms for which k_1 and $k_2 = 1$ or 2 need be included and we obtain the result that

$$W_F{}^{(2)}= \sum_{(\alpha'J')}{}' [W(\alpha J)-W(\alpha'J')]^{-1} \Bigg[\begin{Bmatrix} \tfrac{3}{2} & J' & F \\ J & \tfrac{3}{2} & 1 \end{Bmatrix}^2 \tfrac{20}{3}\mu_I{}^2 \langle \alpha J \| T_e{}^{(1)} \| \alpha'J' \rangle^2$$

$$+ \begin{Bmatrix} \tfrac{3}{2} & J' & F \\ J & \tfrac{3}{2} & 1 \end{Bmatrix} \begin{Bmatrix} \tfrac{3}{2} & J' & F \\ J & \tfrac{3}{2} & 2 \end{Bmatrix} \frac{20}{\sqrt{3}}\mu_I eQ \langle \alpha J \| T_e{}^{(1)} \| \alpha'J' \rangle$$

$$\times \langle \alpha J \| T_e{}^{(2)} \| \alpha'J' \rangle + \begin{Bmatrix} \tfrac{3}{2} & J' & F \\ J & \tfrac{3}{2} & 2 \end{Bmatrix}^2 5e^2Q^2 \langle \alpha J \| T_e{}^{(2)} \| \alpha'J' \rangle^2 \Bigg]. \quad (3)$$

III. EXPERIMENTAL PROCEDURE AND RESULTS

A careful plot of the metastable atomic beam intensity as a function of the bombarder voltage was made initially. As the bombarder voltage is increased from zero, the metastable Au beam intensity (normalized for changes in bombarder current) goes through two maxima. These peaks, at ~5 V and ~10 V, indicate the presence of at least two metastable levels. As shown below, the lower peak corresponds to the production of the $(5d^9 6s^2)$ $^2D_{3/2}$ level. The broader upper peak corresponds to the production of the $(5d^9 6s6p)$ $^4F_{9/2}$ level. As a consequence of the selection rules for electric dipole transitions, these two levels are expected to be the lowest-lying metastable levels in Au (see Fig. 1).

Since $I=\tfrac{3}{2}$ for Au^{197}, each fine-structure level splits into four hfs levels for $J\geq\tfrac{3}{2}$ and into $2J+1$ levels for $J<\tfrac{3}{2}$. In a weak magnetic field, each hfs level then splits into $2F+1$ sublevels. The ratios of the (degenerate) Zeeman splittings $(\Delta E)_F \equiv |E(F, m) - E(F, m\pm1)|$ within each fine-structure level are given by $(\Delta E)_F/(\Delta E)_{F-1}=g_F/g_{F-1}$. By comparing the predicted ratios with the ratios of the observed transitions which were maximized at the bombarder voltage of ~10 V, the identification of the $^4F_{9/2}$ level was made. We also observed, at the higher bombarding voltages, several additional resonances which we were unable to associate with particular F and g_J values. We did not investigate these resonances further. At a bombarder voltage of ~5 V, only one low field $\Delta F=0$ transition was maximized. This indicated that the level

being excited was the $^2D_{3/2}$ level since for $J=I$, $g_F=\tfrac{1}{2}(g_J+g_I)$, independent of F, and only one transition is expected.

The identification of the $^2D_{3/2}$ and $^4F_{9/2}$ levels was corroborated by obtaining g_J values from each of the observed low-field $(\Delta E)_F$ transitions. This was accomplished by using transitions between the Zeeman levels of the metastable $(3s3p)$ $^3P_{2,1}$ states of the zero-spin isotopes of Mg to calibrate the field.

The hfs of the $^2D_{3/2}$ and of the $^4F_{9/2}$ levels is shown schematically as a function of applied magnetic field in Figs. 2 and 3, respectively. The inversion of the $F=3$ and $F=2$ levels had already been deduced from the optical measurements of the hfs by von Siemens.[5]

Estimates for the zero-field separations were obtained by following the $(\Delta E)_F$ transitions up in magnetic field until they were completely resolved. Using standard perturbation theory, the frequencies of these resolved lines can be related to the zero-field hfs. A successful search was then made to observe the $\Delta\nu[(F, m)\leftrightarrow(F-1, m')]$ transitions in such a low magnetic field that all the transitions overlapped. For the $^4F_{9/2}$ level, we made a series of precision measurements of the $\Delta\nu[(F, 0)\leftrightarrow(F-1, 0)]$ σ-transitions since they are field independent to first order. For the $^2D_{3/2}$ level, all the $\Delta\nu[(F, m)\leftrightarrow(F-1, m)]$ σ transitions are degenerate to first order in field and the precision measurements were made on these overlapped transitions in very low fields. The results for the two levels
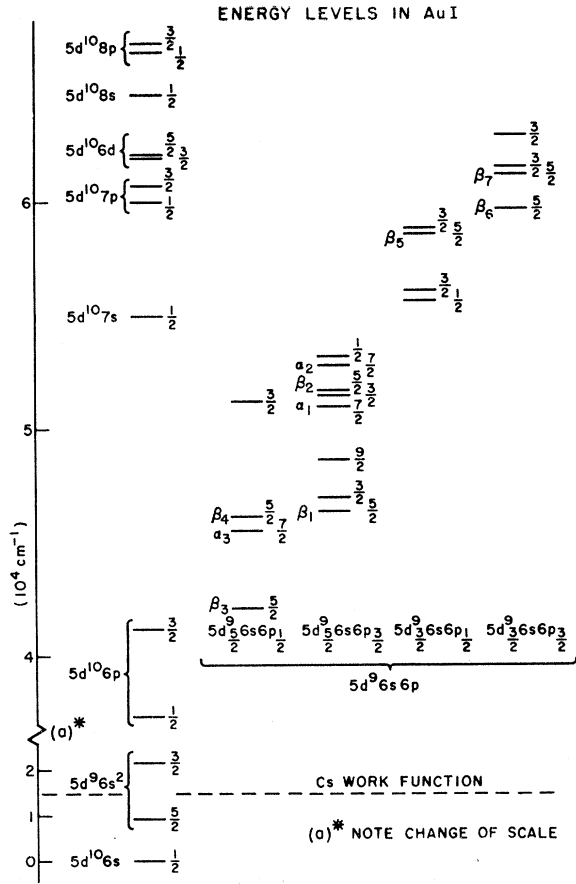
[5] W. v. Siemens, Ann. Physik **13**, 158 (1953).

FIG. 1. Energy-level diagram of the low-lying levels of gold. The quantum number at the right of each level is the J value in that level.

are given in Table I and typical resonance curves are shown in Figs. 4 and 5. After making the small, second-order field-dependent corrections for each line, we obtain the following results for the hfs separations ($\Delta\nu$ is the magnitude of the transition indicated in the parentheses):

$$\Delta\nu(^2D_{3/2};\ F=3\leftrightarrow F=2)=311.5473(2)\ \text{Mc/sec},$$

$$\Delta\nu(^2D_{3/2};\ F=2\leftrightarrow F=1)=1310.7555(12)\ \text{Mc/sec},$$

$$\Delta\nu(^2D_{3/2};\ F=1\leftrightarrow F=0)=1110.9315(5)\ \text{Mc/sec},$$

$$\Delta\nu(^4F_{9/2};\ F=6\leftrightarrow F=5)=2233.7160(14)\ \text{Mc/sec},$$

$$\Delta\nu(^4F_{9/2};\ F=5\leftrightarrow F=4)=2273.8874(6)\ \text{Mc/sec},$$

$$\Delta\nu(^4F_{9/2};\ F=4\leftrightarrow F=3)=2089.1430(4)\ \text{Mc/sec}.$$

The error quoted in each of the above results is three times the standard deviation of the mean of all determinations of that quantity so as to allow for a possible unfavorable accumulation of errors in the relatively small number of runs made.

After these hfs intervals had been measured we re-analyzed the intermediate-field Zeeman data in order to obtain the g_J values for the two states. From this data we find $g_J(^2D_{3/2})=0.799(1)$ and $g_J(^4F_{9/2})=1.334(2)$. These values are in very good agreement with the theoretical values of $g_J(^2D_{3/2})=0.7995$ and $g_J(^4F_{9/2})=1.3341$ obtained by assuming no configuration mixing in the levels.

From the transit time of the Au beam down the apparatus, a lower limit of ~ 1 msec is obtained for the lifetimes of both the $^2D_{3/2}$ and $^4F_{9/2}$ levels.

IV. DISCUSSION OF RESULTS

A. Wave functions

In order to interpret the above results, the electron coupling in the configurations (core) $(5d^96s^2)$ and (core) $(5d^96s6p)$ which give rise to the $^2D_{3/2}$ and $^4F_{9/2}$ levels, respectively, must be investigated. We will treat the problem from a single configuration point of view. Within each configuration, however, we will estimate the second-order contributions to the hfs from nearby fine-structure levels since these are the ones that can give contributions to within the precision of the measurements.
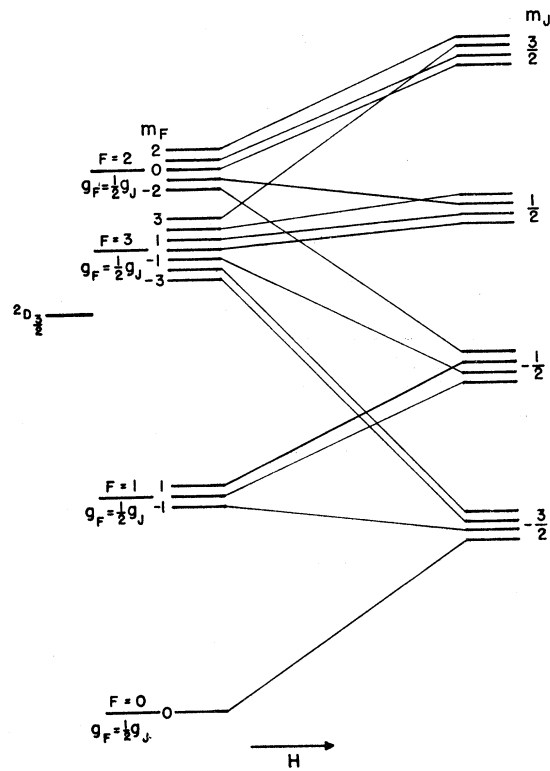

FIG. 2. Hyperfine structure and Zeeman effect of the $^2D_{3/2}$ state of gold. The Zeeman effect is drawn schematically and not shown to scale.

It will be seen that this approach is sufficient to obtain consistency in much of the interpretation of the hfs of the two levels. It appears to be inadequate, however, to give a completely unambiguous value for the magnetic octupole moment of the Au¹⁹⁷ nucleus.

Since the $(5d^9 6s^2)$ $^2D_{3/2}$, $^2D_{5/2}$, and $(5d^9 6s6p)$ $^4F_{9/2}$ levels are the only ones with those J values in their respective configurations, their wave functions are independent of coupling in the single-configuration approximation. The other wave functions of a given J value in the $(5d^9 6s6p)$ configuration can be described by orthogonal superpositions of all the wave functions of that J value obtained from any complete set for the configuration.

TABLE I. Experimental hfs data and results for Au¹⁹⁷.
(All units are Mc/sec.)

State	F	$\mid \Delta\nu[(F,0)\leftrightarrow(F-1,0)]\mid$	$\mu_0 H$	$\mid \Delta\nu[F\leftrightarrow F-1]\mid$
$^2D_{3/2}$	3	311.5475	0.283	311.5473
		311.5477	0.280	311.5475
		311.5474	0.278	311.5472
$^2D_{3/2}$	2	1310.7545	0.251	1310.7544
		1310.7547	0.246	1310.7546
		1310.7555	0.244	1310.7554
		1310.7564	0.240	1310.7563
		1310.7568	0.238	1310.7567
$^2D_{3/2}$	1	1110.9321	0.227	1110.9320
		1110.9315	0.225	1110.9314
		1110.9314	0.222	1110.9313
		1110.9313	0.219	1110.9312
$^4F_{9/2}$	6	2233.7339	9.06	2233.7159
		2233.7160	1.12	2233.7157
		2233.7168	1.13	2233.7165
		2233.7180	1.78	2233.7173
		2233.7148	1.13	2233.7145
$^4F_{9/2}$	5	2273.8887	1.78	2273.8879
		2273.8883	1.78	2273.8875
		2273.8874	1.78	2273.8866
		2273.8879	0.86	2273.8877
		2273.9072	9.00	2273.8871
$^4F_{9/2}$	4	2089.2087	8.99	2089.1433
		2089.1439	1.45	2089.1430
		2089.1505	3.09	2089.1428

As can be seen from the energy-level diagram shown in Fig. 1, the levels are divided into two groups (which are based, according to Platt and Sawyer,[6] on the $(5d^9)$ $^2D_{3/2}$ and $^2D_{5/2}$ levels of Au III). This results from the fact that the Au spectrum exhibits approximate j–j coupling.[6] (Note that three of the levels that would fall into the upper group have not yet been observed.) The j value assignments for the individual electrons for each level were made by Trees and Moore[7] on the basis of a comparison of the observed g factors with those calculated by assuming that the j–j coupling is

[6] J. R. Platt and R. A. Sawyer, Phys. Rev. **60**, 866 (1941).
[7] C. E. Moore, *Atomic Energy Level*, edited by C. E. Moore, Natl. Bur. Std. (U.S.) Circ. No. 467 (U.S. Government Printing Office, Washington, D.C., 1958).
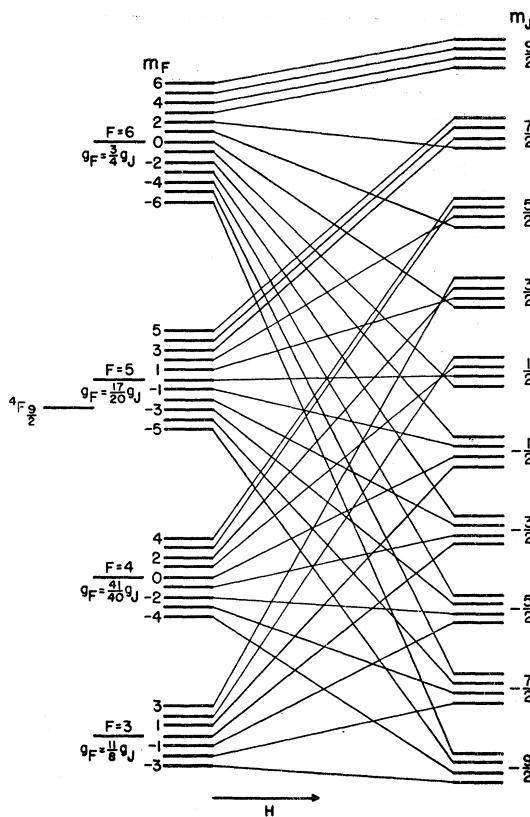

FIG. 3. Hyperfine structure and Zeeman effect of the $^4F_{9/2}$ state of gold. The Zeeman effect is drawn schematically and not shown to scale.
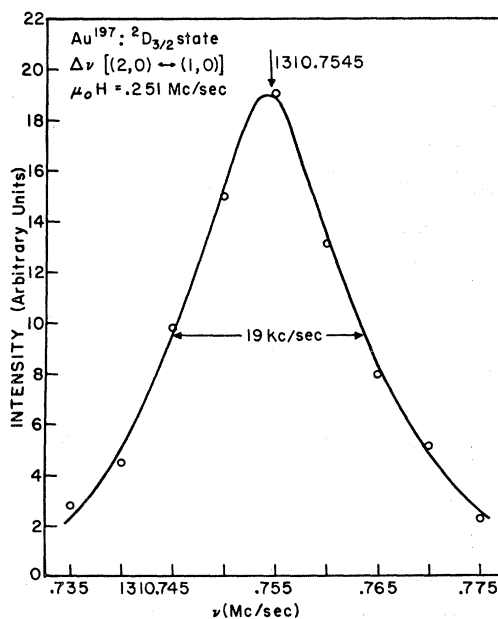

FIG. 4. Typical curve obtained for the $\Delta\nu[(2,0)\leftrightarrow(1,0)]$ field-independent transition in the $^2D_{3/2}$ state.
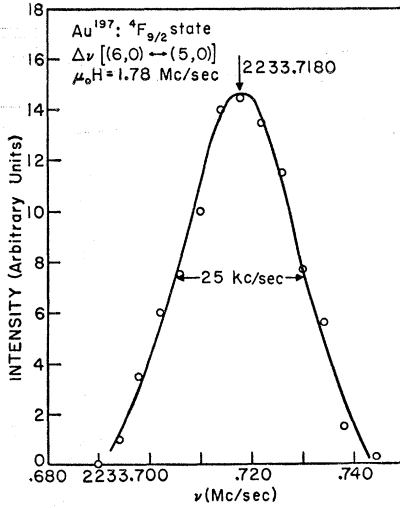
FIG. 5. Typical curve obtained for the $\Delta\nu[(6, 0) \leftrightarrow (5, 0)]$ field-independent transition in the $^4F_{9/2}$ state.

in the order $(((d^9)s)p)$. Their results are reproduced in Table II and, as can be seen, there is general agreement. (In the table, dashes indicate that the level is known but no observed g factor is available. The three levels marked "absent" are the levels as yet unobserved.) A further detailed analysis of the structure of these levels would be prohibitively difficult in view of the missing levels together with the general complexity of the spectrum. Inasmuch as the gross structure of the configuration can be successfully described by the $(((d^9)s)p)$ j-j coupling scheme, we will assume that the eigenstates can be approximated by the corresponding wave functions.

B. The hfs Interaction Constants

From Eq. 2, the zero-field hfs intervals can be written as follows, where $\Delta\nu$ is the magnitude of the hfs interval:

$$\Delta\nu(^2D_{3/2}; F=3 \leftrightarrow F=2) = -3A(^2D_{3/2}) - B(^2D_{3/2})$$
$$-8C(^2D_{3/2}) + h^{-1}[W_2^{(2)}(^2D_{3/2}) - W_3^{(2)}(^2D_{3/2})],$$

$$\Delta\nu(^2D_{3/2}; F=2 \leftrightarrow F=1) = 2A(^2D_{3/2}) - B(^2D_{3/2})$$
$$-28C(^2D_{3/2}) + h^{-1}[W_2^{(2)}(^2D_{3/2}) - W_1^{(2)}(^2D_{3/2})],$$

$$\Delta\nu(^2D_{3/2}; F=1 \leftrightarrow F=0) = A(^2D_{3/2}) - B(^2D_{3/2})$$
$$+56C(^2D_{3/2}) + h^{-1}[W_1^{(2)}(^2D_{3/2}) - W_0^{(2)}(^2D_{3/2})],$$

$$\Delta\nu(^4F_{9/2}; F=6 \leftrightarrow F=5) = 6A(^4F_{9/2}) + \tfrac{2}{3}B(^4F_{9/2})$$
$$+\tfrac{16}{3}C(^4F_{9/2}) + h^{-1}[W_6^{(2)}(^4F_{9/2}) - W_5^{(2)}(^4F_{9/2})],$$

$$\Delta\nu(^4F_{9/2}; F=5 \leftrightarrow F=4) = 5A(^4F_{9/2}) - \tfrac{5}{24}B(^4F_{9/2})$$
$$-\tfrac{65}{6}C(^4F_{9/2}) + h^{-1}[W_5^{(2)}(^4F_{9/2}) - W_4^{(2)}(^4F_{9/2})],$$

$$\Delta\nu(^4F_{9/2}; F=4 \leftrightarrow F=3) = 4A(^4F_{9/2}) - \tfrac{2}{3}B(^4F_{9/2})$$
$$+\tfrac{208}{21}C(^4F_{9/2}) + h^{-1}[W_4^{(2)}(^4F_{9/2}) - W_3^{(2)}(^4F_{9/2})]. \quad (4)$$

Neglecting the second-order terms, we have

$$A(^2D_{3/2}) = 199.8425(2) \text{ Mc/sec},$$

$$B(^2D_{3/2}) = -911.0766(5) \text{ Mc/sec},$$

$$C(^2D_{3/2}) = 0.000221(14) \text{ Mc/sec},$$

$$A(^4F_{9/2}) = 432.2827(1) \text{ Mc/sec},$$

$$B(^4F_{9/2}) = -539.9869(11) \text{ Mc/sec},$$

$$C(^4F_{9/2}) = 0.00213(4) \text{ Mc/sec}.$$

Evaluation of the relevant matrix elements allows the hfs constants and second-order energy terms to be expressed in terms of contributions from the individual valence electrons. We have

$$A(^2D_{3/2}) = a(d_{3/2}),$$

$$B(^2D_{3/2}) = -b(d_{3/2}),$$

$$C(^2D_{3/2}) = c(d_{3/2}),$$

$$A(^4F_{9/2}) = \tfrac{1}{9}a(s) + \tfrac{1}{3}a(p_{3/2}) + \tfrac{5}{9}a(d_{5/2}),$$

$$B(^4F_{9/2}) = b(p_{3/2}) - b(d_{5/2}),$$

$$C(^4F_{9/2}) = c(p_{3/2}) + c(d_{5/2}), \quad (5)$$

where the single-electron hfs interaction constants are given by

$$a(l_j) = (2\mu_I/3j) \langle \tfrac{1}{2}ljj \mid T_e^{(1)}{}_0 \mid \tfrac{1}{2}ljj \rangle$$
$$= \tfrac{8}{9}\mu_0\mu_I \mid R(0) \mid^2 F_r(0, \tfrac{1}{2}, Z_i)(1-\delta)(1-\epsilon)$$
$$\text{for } l=0,$$
$$= \tfrac{4}{3}\mu_0\mu_I \frac{l(l+1)}{j(j+1)} \langle r^{-3} \rangle F_r(l, j, Z_i)(1-\delta)(1-\epsilon)$$
$$\text{for } l>0, \quad (6)$$

$$b(l_j) = 2eQ \langle \tfrac{1}{2}ljj \mid T_e^{(2)}{}_0 \mid \tfrac{1}{2}ljj \rangle$$
$$= [(2j-1)/(2j+2)]e^2 Q \langle r^{-3} \rangle R_r(l, j, Z_i), \quad (7)$$

$$c(l_j) = -\Omega \langle \tfrac{1}{2}ljj \mid T_e^{(3)}{}_0 \mid \tfrac{1}{2}ljj \rangle$$
$$= 0 \qquad\qquad \text{for } j=\tfrac{1}{2},$$
$$= \tfrac{4}{35}\mu_0\Omega \left| \frac{R(r)}{r} \right|^2_{r=0} T_r(1, \tfrac{3}{2}, Z_i)$$
$$\text{for } l=1, j=\tfrac{3}{2},$$
$$= \frac{2l(l-1)(l+1)(l+2)}{(j+1)(j+2)(2j+3)} \mu_0\Omega \langle r^{-5} \rangle T_r(l, j, Z_i)$$
$$\text{for } l>1. \quad (8)$$

In these expressions, $R(r)$ is the normalized radial part of the electronic wave function, F_r, R_r, and T_r [4,8] are relativistic correction factors, Z_i is the effective nuclear charge, and the factors $(1-\delta)$ and $(1-\epsilon)$ are corrections for the volume distribution of nuclear charge

[8] H. Kopfermann, *Nuclear Moments* (Academic Press Inc., New York, 1958).

HYPERFINE STRUCTURE OF Au[197]

TABLE II. Theoretical and observed g_J values for the $(5d)^9 6s6p$ configuration of gold. The theoretical g_J values are calculated assuming jj coupling.[a]

Term	J	9/2	7/2	5/2	3/2	1/2
$(5d_{5/2})^9 6s_{1/2} 6p_{3/2}$						
$5d^9 6s(J=3)6p_{3/2}$	Theory	1.333	1.333	1.333	1.333	
	Observed	•••	1.372	•••	1.422	
$5d^9 6s(J=2)6p_{3/2}$	Theory		1.181	1.166	1.120	0.800
	Observed		•••	1.222	•••	•••
$(5d_{5/2})^9 6s_{1/2} 6p_{1/2}$						
$5d^9 6s(J=3)6p_{1/2}$	Theory		1.238	1.429		
	Observed		1.258	1.532		
$5d^9 6s(J=2)6p_{1/2}$	Theory			0.987	1.147	
	Observed			1.011	1.064	
$(5d_{3/2})^9 6s_{1/2} 6p_{3/2}$						
$5d^9 6s(J=2)6p_{3/2}$	Theory		1.200	1.187	1.147	0.867
	Observed		Absent	1.30	•••	Absent
$5d^9 6s(J=1)6p_{3/2}$	Theory			1.000	1.111	1.889
	Observed			•••	•••	Absent
$(5d_{3/2})^9 6s_{1/2} 6p_{1/2}$						
$5d^9 6s(J=2)6p_{1/2}$	Theory			1.013	1.187	
	Observed			0.984	1.16	
$5d^9 6s(J=1)6p_{1/2}$	Theory				0.556	0.444
	Observed				•••	•••

[a] See Ref. 7, Vol. III, p. 187.

and current, respectively. The matrix elements needed to calculate the various contributions to $W_F{}^{(2)}$ are given in the Appendix.

The following procedure was used to estimate the single-electron coupling constants. Values of $a(d_{5/2})$ and $b(d_{3/2})$ for the $^2D_{3/2}$ level can be obtained by ignoring the small second-order corrections to $A(^2D_{3/2})$ and $B(^2D_{3/2})$, respectively. With these uncorrected hfs interaction constants the second-order energy corrections are obtained from Eq. (3) and substitution of the results into Eqs. (4) gives the corrected hfs interaction constants. (One such iteration was found to be sufficient.) The corrections to $A(^2D_{3/2})$ and $B(^2D_{3/2})$ are negligible to within the uncertainty in the first-order values but $C(^2D_{3/2})$ is changed, its corrected value being

$$C(^2D_{3/2}) = 0.000212(14)\,\mathrm{Mc/sec}.$$

To obtain the single-electron coupling constants for the $^4F_{9/2}$ level we can use Eqs. (6) and (7) to give the relations

$$\frac{b(p_{3/2})}{a(p_{3/2})} = -3\,\frac{R_r(1,\frac{3}{2},75)}{R_r(2,\frac{3}{2},69)}\,\frac{F_r(2,\frac{3}{2},69)}{F_r(1,\frac{3}{2},75)}\,\frac{B(^2D_{3/2})}{A(^2D_{3/2})} = 13.1,$$

$$\frac{b(d_{5/2})}{a(d_{5/2})} = -\frac{10}{3}\,\frac{R_r(2,\frac{5}{2},69)}{R_r(2,\frac{3}{2},69)}\,\frac{F_r(2,\frac{3}{2},69)}{F_r(2,\frac{5}{2},69)}\,\frac{B(^2D_{3/2})}{A(^2D_{3/2})} = 13.4,$$

where $Z_i = Z-4$ and $Z-10$ for a p and d electron,

respectively.[8,9] Together with Eqs. (5), then, we have two equations with three unknowns which we can take to be $a(s)$, $a(p_{3/2})$, and $a(d_{5/2})$. These unknowns can be estimated separately from the measured hfs of the $(5d^{10}6s)\ ^2S_{1/2}$ ground level,[10] the $(5d^{10}6p)\ ^2P_{1/2}$ level,[5] and the $(5d^9 6s^2)\ ^2D_{3/2,5/2}$ levels,[9] respectively. Assuming such a value for each of the a's in turn we get three cases, the results for which are shown in Table III. ΔA, ΔB, and ΔC are the corrections to the hfs interaction constants and, except for ΔB case i, each is substantially the same for the three cases. In these calculations, we have neglected the possibility of a near degeneracy ($|\ W(^4F_{9/2}) - W(\alpha_4\frac{7}{2})\ | \lesssim 500\ \mathrm{cm}^{-1}$) of the unobserved $J = \frac{7}{2}$ level with the $^4F_{9/2}$ level. The state $|\ \alpha_4\frac{7}{2}\ \rangle$ is defined in the Appendix. The general structure of the configuration makes this unlikely, however. Taking the average for each correction, the corrected hfs interaction constants are

$$A(^4F_{9/2}) = 432.276(1)\ \mathrm{Mc/sec},$$

$$B(^4F_{9/2}) = -540.026(17)\ \mathrm{Mc/sec},$$

$$C(^4F_{9/2}) = 0.00326(10)\ \mathrm{Mc/sec}.$$

[9] The proper choice of Z_i is discussed by W. J. Childs and L. S. Goodman, Phys. Rev. 141, 176 (1966).

[10] E. Recknagel, Z. Physik 159, 19 (1960); G. Wessel and H. Lew, Phys. Rev. 92, 641 (1953).

TABLE III. The individual-electron hfs interaction constants and second-order energy corrections. (All units are Mc/sec.) Case i: $a(s)$ estimated from $(5d^{10}6s)$ $^2S_{1/2}$ level hfs. Case ii: $a(p_{3/2})$ estimated from $(5d^{10}6p)$ $^2P_{1/2}$ level hfs. Case iii: $a(d_{5/2})$ estimated from $(5d^96s^2)$ $^2D_{3/2,5/2}$ level hfs.

	i	ii	iii
$a(s)$	3050	3389	3365
$a(p_{3/2})$	81	38	41
$b(p_{3/2})$	1058	497	536
$a(d_{5/2})$	120	78	80
$b(d_{5/2})$	1598	1037	1076
ΔA $(^4F_{9/2})$ [a]	−0.0063	−0.0063	−0.0055
ΔB $(^4F_{9/2})$ [b]	−0.0184	−0.0528	−0.0504
ΔC $(^4F_{9/2})$ [c]	0.00107	0.00120	0.00112

[a] ΔA $(^4F_{9/2}) \equiv A$ $(^4F_{9/2})$ (corrected) $-A$ $(^4F_{9/2})$ (first order).
[b] $\Delta B(^4F_{9/2}) \equiv B(^4F_{9/2})$ (corrected) $-B(^4F_{9/2})$ (first order).
[c] ΔC $(^4F_{9/2}) \equiv C$ $(^4F_{9/2})$ (corrected) $-C$ $(^4F_{9/2})$ (first order).

The major source of error in the above values lies in the uncertainty in the electron coupling within the configuration together with the neglect of any inter-configuration mixing.

An analysis of the $(5d^96s^2)$ ^2D term hfs has been presented by Childs and Goodman[9] who measured the hfs of the $(5d^96s^2)$ $^2D_{5/2}$ level. As they have shown, the values of the A constants and the ratio of the B constants for the two levels are in good agreement with those predicted from the known values of μ_I and $\langle r^{-3} \rangle_{5d}$, the latter being obtained from the fine-structure splitting of the ^2D term. This indicates that the ^2D term arises almost completely from the $(5d^96s^2)$ configuration and therefore that core polarization effects should be small for these levels.

C. The Nuclear Electric Quadrupole Moment

The value of the nuclear electric quadrupole moment can be obtained from the ratio $B(^2D_{3/2})/A(^2D_{3/2})$:

$$Q = -\frac{16}{3}\frac{\mu_0\mu_I}{e^2}(1-\delta)(1-\epsilon)\frac{F_r(2,\frac{3}{2},69)}{R_r(2,\frac{3}{2},69)}\frac{B(^2D_{3/2})}{A(^2D_{3/2})}$$

$$= 0.604 \times 10^{-24} \text{ cm}^2.$$

The corresponding result calculated from the $^2D_{5/2}$ level hfs is given by Goodman and Childs to be

$$Q = 0.585 \times 10^{-24} \text{ cm}^2.$$

Averaging the above values gives

$$Q = 0.594(10) \times 10^{-24} \text{ cm}^2.$$

This quadrupole moment does not include the Sternheimer correction.[11]

D. The Nuclear Magnetic Octupole Moment

From the expressions for the radial integrals derived by Schwartz,[4] we can relate $c(l_j)$ to $a(l_j)$ and obtain the following equations for the nuclear magnetic octupole moment.

(i) From the $^2D_{3/2}$ level hfs:

$$\Omega = \frac{147}{5}\frac{\mu_I}{I}\left(\frac{a_0}{Z}\right)^2\frac{F_r(2,\frac{3}{2},Z)}{T_r(2,\frac{3}{2},Z)}\frac{c(d_{3/2})}{a(d_{3/2})}$$

$$= 0.0098(7) \times 10^{-24} \text{ nm cm}^2.$$

(ii) From the $^2D_{5/2}$ level hfs [we have taken the values of $c(d_{5/2})$ and $a(d_{5/2})$ from Goodman and Childs]:

$$\Omega = \frac{756}{25}\frac{\mu_I}{I}\left(\frac{a_0}{Z}\right)^2\frac{F_r(2,\frac{5}{2},Z)}{T_r(2,\frac{5}{2},Z)}\frac{c(d_{5/2})}{a(d_{5/2})}$$

$$= 0.06(6) \times 10^{-24} \text{ nm cm}^2.$$

(iii) From the $^4F_{9/2}$ level hfs: In this case we use the value of $c(d_{3/2})$ obtained from the $^2D_{3/2}$ level hfs to estimate $c(d_{5/2}) = 0.000065$ Mc/sec. Subtracting this from the corrected value of $C(^4F_{9/2})$ gives

$$c(p_{3/2}) = 0.00319 \text{ Mc/sec.}$$

The expression for Ω is

$$\Omega = 7\frac{\mu_I}{I}\left(\frac{a_0}{Z}\right)^2\frac{F_r(1,\frac{3}{2},Z)}{T_r(1,\frac{3}{2},Z)}\frac{c(p_{3/2})}{a(p_{3/2})} = 0.13 \times 10^{-24} \text{ nm cm}^2,$$

where the average of the three values of $a(p_{3/2})$ given in Table III was used. $Z = 79$ was used in the above calculations. The choice of Z in these calculations is very uncertain. If one were to use $Z = 69$ then the values for the octupole moment would become: (i) $\Omega = 0.014(1) \times 10^{-24}$ nm cm², (ii) $\Omega = 0.08(8) \times 10^{-24}$ nm cm², and (iii) $\Omega = 0.18 \times 10^{-24}$ nm cm². The errors quoted in cases (i) and (ii) include only experimental errors.

As noted above, the analysis of the A and B factors for the $^2D_{3/2}$ and $^2D_{5/2}$ levels by Goodman and Childs fails to reveal the presence of any configuration mixing in the ^2D term. It follows that core polarization corrections to the values for Ω obtained for cases (i) and (ii) should be small and hence that these values should be relatively reliable. The fact that these values agree within the stated errors lends support to the conclusion.

[11] R. M. Sternheimer, Phys. Rev. **80**, 102 (1950); **84**, 244 (1951); **86**, 316 (1952); **95**, 736 (1954); **105**, 158 (1957).

The value for Ω obtained from the $^4F_{9/2}$ level hfs is roughly an order of magnitude larger than the D state results. There are, however, several possible causes for this disagreement.[4] Firstly, there is the approximate nature of the theory relating $a(l_j)$ to $c(l_j)$. Secondly, the uncertainties in the values of $a(p_{3/2})$ and $c(p_{3/2})$ are large. The spread in $a(p_{3/2})$ in Table III indicates an uncertainty of $\sim50\%$ in its average value. In addition, the deviation from the assumed $(((d^9)s)p)$ j-j coupling scheme within the configuration must be taken into account. Thirdly, there is a possibility of a near degeneracy of the unobserved $J=\frac{7}{2}$ level with the $^4F_{9/2}$ level. Fourthly, core polarization (i.e., configuration mixing) corrections may be considerable. A satisfactory analysis of these possible sources of discrepancy requires an analysis of the Au spectrum that is much more complete, however, than that which is at present available.

The smaller value of Ω is supported by the fact that the nuclear magnetic dipole and electric quadrupole moments are fairly well predicted by the hypothesis that they arise entirely from a $2d_{3/2}^{-1}$ proton configuration.[12] The corresponding prediction for Ω is -0.025×10^{-24} nm cm^2 [assuming $\langle r^2\rangle_{\text{nucleus}}\sim\frac{3}{5}(0.135A^{1/3})^2\times10^{-24}$ cm^2], favoring the value obtained from the $^2D_{3/2}$ level measurements.

APPENDIX

The following notation will be used to describe the wave functions for the various j-j coupled levels of the $(5d^96s6p)$ configuration:

$$|\,\alpha Jm\,\rangle = |\,(J_1,\,J_2)\,J_{12},\,J_3;\,Jm\,\rangle.$$

J_1 denotes the resultant angular momentum of the unfilled group of equivalent d electrons, J_2 and J_3 denote, respectively, the angular momentum of the s and p electrons, J_{12} denotes the values obtained by coupling J_1 and J_2, and J denotes the total angular momentum of the state obtained by coupling J_{12} and J_3. Since these couplings involve nonequivalent groups of electrons, all vector coupling values of J_{12} and J are allowed. The various levels are also distinguished by the labels α_i and β_i to facilitate their identification in Fig. 1.

---

[12] E. Feenberg, *Shell Theory of the Nucleus* (Princeton University Press, Princeton, New Jersey, 1955), p. 48.

We have:

$$|\,\alpha_1\tfrac{7}{2}m\,\rangle = |\,(\tfrac{5}{2},\tfrac{1}{2})3,\tfrac{3}{2};\tfrac{7}{2}m\,\rangle,$$

$$|\,\alpha_2\tfrac{7}{2}m\,\rangle = |\,(\tfrac{5}{2},\tfrac{1}{2})2,\tfrac{3}{2};\tfrac{7}{2}m\,\rangle,$$

$$|\,\alpha_3\tfrac{7}{2}m\,\rangle = |\,(\tfrac{5}{2},\tfrac{1}{2})3,\tfrac{1}{2};\tfrac{7}{2}m\,\rangle,$$

$$|\,\alpha_4\tfrac{7}{2}m\,\rangle = |\,(\tfrac{3}{2},\tfrac{1}{2})2,\tfrac{3}{2};\tfrac{7}{2}m\,\rangle,$$

$$|\,\beta_1\tfrac{5}{2}m\,\rangle = |\,(\tfrac{5}{2},\tfrac{1}{2})3,\tfrac{3}{2};\tfrac{5}{2}m\,\rangle,$$

$$|\,\beta_2\tfrac{5}{2}m\,\rangle = |\,(\tfrac{5}{2},\tfrac{1}{2})2,\tfrac{3}{2};\tfrac{5}{2}m\,\rangle,$$

$$|\,\beta_3\tfrac{5}{2}m\,\rangle = |\,(\tfrac{5}{2},\tfrac{1}{2})3,\tfrac{1}{2};\tfrac{5}{2}m\,\rangle,$$

$$|\,\beta_4\tfrac{5}{2}m\,\rangle = |\,(\tfrac{5}{2},\tfrac{1}{2})2,\tfrac{1}{2};\tfrac{5}{2}m\,\rangle,$$

$$|\,\beta_5\tfrac{5}{2}m\,\rangle = |\,(\tfrac{3}{2},\tfrac{1}{2})2,\tfrac{1}{2};\tfrac{5}{2}m\,\rangle,$$

$$|\,\beta_6\tfrac{5}{2}m\,\rangle = |\,(\tfrac{3}{2},\tfrac{1}{2})1,\tfrac{3}{2};\tfrac{5}{2}m\,\rangle,$$

$$|\,\beta_7\tfrac{5}{2}m\,\rangle = |\,(\tfrac{3}{2},\tfrac{1}{2})2,\tfrac{3}{2};\tfrac{5}{2}m\,\rangle.$$

The relevant matrix elements are then given in terms of the single-electron coupling constants as follows:

$$\langle\tfrac{9}{2}\,||\,T_e^{(1)}\,||\,\alpha_1\tfrac{7}{2}\rangle = \tfrac{1}{2}(\tfrac{5}{2})^{1/2}[a(s)-6a(p_{3/2})\\+5a(d_{5/2})]\mu_I^{-1},$$

$$\langle\tfrac{9}{2}\,||\,T_e^{(1)}\,||\,\alpha_2\tfrac{7}{2}\rangle = -\tfrac{5}{2}(\tfrac{3}{2})^{1/2}[a(s)-a(d_{5/2})]\mu_I^{-1},$$

$$\langle\tfrac{9}{2}\,||\,T_e^{(1)}\,||\,\alpha_3\tfrac{7}{2}\rangle = -\tfrac{15}{16}(\tfrac{15}{2})^{1/2}\xi(p)a(p_{3/2})\mu_I^{-1},$$

$$\langle\tfrac{9}{2}\,||\,T_e^{(1)}\,||\,\alpha_4\tfrac{7}{2}\rangle = -\tfrac{35}{16}\xi(d)a(d_{5/2})\mu_I^{-1},$$

$$\langle\tfrac{9}{2}\,||\,T_e^{(2)}\,||\,\alpha_1\tfrac{7}{2}\rangle = -(\tfrac{110}{21})^{1/2}[b(p_{3/2})+\tfrac{1}{2}b(d_{5/2})]Q^{-1},$$

$$\langle\tfrac{9}{2}\,||\,T_e^{(2)}\,||\,\alpha_2\tfrac{7}{2}\rangle = (\tfrac{11}{14})^{1/2}b(d_{5/2})Q^{-1},$$

$$\langle\tfrac{9}{2}\,||\,T_e^{(2)}\,||\,\alpha_3\tfrac{7}{2}\rangle = -(\tfrac{55}{14})^{1/2}\eta(p)b(p_{3/2})Q^{-1},$$

$$\langle\tfrac{9}{2}\,||\,T_e^{(2)}\,||\,\alpha_4\tfrac{7}{2}\rangle = -\tfrac{1}{2}(\tfrac{33}{7})^{1/2}\eta(d)b(d_{5/2})Q^{-1},$$

$$\langle\tfrac{9}{2}\,||\,T_e^{(2)}\,||\,\beta_1\tfrac{5}{2}\rangle = \tfrac{1}{2}(\tfrac{3}{7})^{1/2}[5b(p_{3/2})-b(d_{5/2})]Q^{-1},$$

$$\langle\tfrac{9}{2}\,||\,T_e^{(2)}\,||\,\beta_2\tfrac{5}{2}\rangle = -(\tfrac{3}{14})^{1/2}b(d_{5/2})Q^{-1},$$

$$\langle\tfrac{9}{2}\,||\,T_e^{(2)}\,||\,\beta_3\tfrac{5}{2}\rangle = 2(\tfrac{15}{7})^{1/2}\eta(p)b(p_{3/2})Q^{-1},$$

$$\langle\tfrac{9}{2}\,||\,T_e^{(2)}\,||\,\beta_4\tfrac{5}{2}\rangle = 0,$$

$$\langle\tfrac{9}{2}\,||\,T_e^{(2)}\,||\,\beta_5\tfrac{5}{2}\rangle = 0,$$

$$\langle\tfrac{9}{2}\,||\,T_e^{(2)}\,||\,\beta_6\tfrac{5}{2}\rangle = \tfrac{1}{2}\eta(d)b(d_{5/2})Q^{-1},$$

$$\langle\tfrac{9}{2}\,||\,T_e^{(2)}\,||\,\beta_7\tfrac{5}{2}\rangle = \tfrac{3}{2}(\tfrac{1}{7})^{1/2}\eta(d)b(d_{5/2})Q^{-1}.$$

ξ and η are relativistic correction factors (~1).[4]

For the $(5d^96s^2)$ $^2D_{5/2,3/2}$ levels we have

$$\langle^2D_{5/2}\,||\,T_e^{(1)}\,||\,^2D_{3/2}\rangle = -\mu_I^{-1}\tfrac{7}{16}(15)^{1/2}\xi a(d_{5/2}),$$

$$\langle^2D_{5/2}\,||\,T_e^{(2)}\,||\,^2D_{3/2}\rangle = Q^{-1}\tfrac{1}{2}(\tfrac{21}{5})^{1/2}\eta b(d_{5/2}).$$